J|A|C|S
ARTICLES
Published on Web 08/31/2006

Lipids Out of Equilibrium: Energetics of Desorption and Pore Mediated Flip-Flop

D. Peter Tieleman*,† and Siewert-Jan Marrink*,‡

Contribution from the Department of Biological Sciences, University of Calgary, 2500 University Drive NW, Calgary, AB T2N 1N4 Canada, and Department of Chemistry, University of Groningen, Nijenborgh 4, 9747 AG Groningen, The Netherlands

Received April 8, 2006; E-mail: tieleman@ucalgary.ca; s.j.marrink@rug.nl

Abstract: The potential of mean force (PMF) of a phospholipid in a bilayer is a key thermodynamic property that describes the energetic cost of localized lipid defects. We have calculated the PMF by umbrella sampling using molecular dynamics simulations. The profile has a deep minimum at the equilibrium position in the bilayer and steeply rises for displacements both deeper into the bilayer and moving away from the bilayer. As the lipid loses contact with the bilayer, the profile abruptly flattens without a significant barrier. The calculated free energy difference of 80 kJ/mol between the minimum of the PMF and the value in water agrees well with the free energy difference calculated from the experimentally measured critical micelle concentration. Significant water/lipid defects form when a lipid is forced into the bilayer interior, in the form of a small water pore that spans the membrane. The energy required to form such a water pore is also found to be 80 kJ/mol. On the basis of this energy, we estimate the lipid flip-flop rate and permeability rate of sodium ions. The resulting rates are in good agreement with experimental measurements, suggesting lipid flip-flop and basal permeability of ions are pore mediated.

Introduction

The potential of mean force (PMF) of phospholipids in a lipid bilayer measures the free energy cost of moving a lipid over a specific distance away from its equilibrium position in the membrane. It therefore is an important property of lipid bilayers that determines the extent of thermal structural fluctuations of a single lipid in the bilayer. Such fluctuations are important in the interactions between membranes through protrusions,[1,2] defects in early stages of fusion,[3,4] enzyme action on lipid bilayers,[5] the strength of lipid anchors,[6−8] lipid transfer by phospholipid transfer proteins,[9] in lipoprotein complexes,[10] trafficking,[11] unassisted lipid flip-flop,[12,13] and transport of polar or charged molecules in membranes that lack specific protein transporters for such molecules.[12−15] The lipid PMF also plays a role in the interpretation of surface force apparatus and other experiments in which one or more lipids are pulled from a membrane to measure the microscopic mechanical properties of lipids.[2,16] The interpretation of such experiments requires an estimate of the potential of mean force to convert between the rupture force and adhesion energies. In simulations, the excess chemical potential of a surfactant provides a link between computational models and experimentally measurable critical micelle concentrations.[2] This allows both testing of force fields and parametrization of new surfactant models to reproduce thermodynamic properties of lipid bilayers and other aggregates of amphipathic molecules in general.

In this study we have calculated the potential of mean force of a dipalmitoyl-phosphatidylcholine (DPPC) lipid in a DPPC bilayer using molecular dynamics simulation. From the PMF, we obtain the solubility of a lipid in good agreement with the critical micelle concentration. Thus the PMF provides a measure for the likelihood of spontaneous lipid fluctuations. When a lipid is constrained in the center of the membrane, small pores form. From the PMF, we can therefore calculate the equilibrium pore density. Combining the pore density with results from other simulations we estimate lipid flip-flop rates and permeation rates of ions. Our results support the interpretation of flip-flop and ion permeation measurements that predicted the occurrence of pore defects as part of the flip-flop mechanism.[12,15,17]

Methods

The simulation system consists of 64 DPPC lipids and 3846 SPC water molecules.[18] The potential of mean force was calculated using umbrella sampling.[19] The umbrella potential acts on the center of mass

† University of Calgary.
‡ University of Groningen.

(1) Brannigan, G.; Brown, F. L. *Biophys. J.* **2006**, *90*, 1501−1520.
(2) Israelachvili, J. *Intermolecular and Surface Forces;* Wiley: New York, 1992.
(3) Marrink, S. J.; Mark, A. E. *J. Am. Chem. Soc.* **2003**, *125*, 11144−11145.
(4) Stevens, M. J.; Hoh, J. H.; Woolf, T. B. *Phys. Rev. Lett.* **2003**, *91*, 188102.
(5) Berg, O. G.; Gelb, M. H.; Tsai, M. D.; Jain, M. K. *Chem. Rev.* **2001**, *101*, 2613−2653.
(6) Maurer-Stroh, S.; Eisenhaber, F. *Trends Microbiol.* **2004**, *12*, 178−185.
(7) Englund, P. T. *Annu. Rev. Biochem.* **1993**, *62*, 121−138.
(8) Sefton, B. M.; Buss, J. E. **1987**, *104*, 1449−1453.
(9) Tall, A. R. *J. Lipid Res.* **1986**, *27*, 361−367.
(10) Mahley, R. W.; Innerarity, T. L.; Rall, S. C.; Weisgraber, K. H. *J. Lipid Res.* **1984**, *25*, 1277−1294.
(11) Gumperz, J. E. *Traffic (Oxford, U.K.)* **2006**, *7*, 2−13.
(12) Kornberg, R. D.; McConnell, H. M. *Biochem.* **1971**, *10*, 1111−20.
(13) de Vries, A. H.; Mark, A. E.; Marrink, S. J. *J. Am. Chem. Soc.* **2004**, *126*, 4488−4489.
(14) Deamer, D. W.; Bramhall, J. *Chem. Phys. Lipids* **1986**, *40*, 167−188.
(15) Toyoshima, Y.; Thompson, T. E. *Biochem.* **1975**, *14*, 1525−1531.
(16) Evans, E.; Ritchie, K.; Merkel, R. *Biophys. J.* **1995**, *68*, 2580−2587.
(17) Wimley, W. C.; Thompson, T. E. *Biochem.* **1991**, *30*, 1702−1709.

10.1021/ja0624321 CCC: $33.50

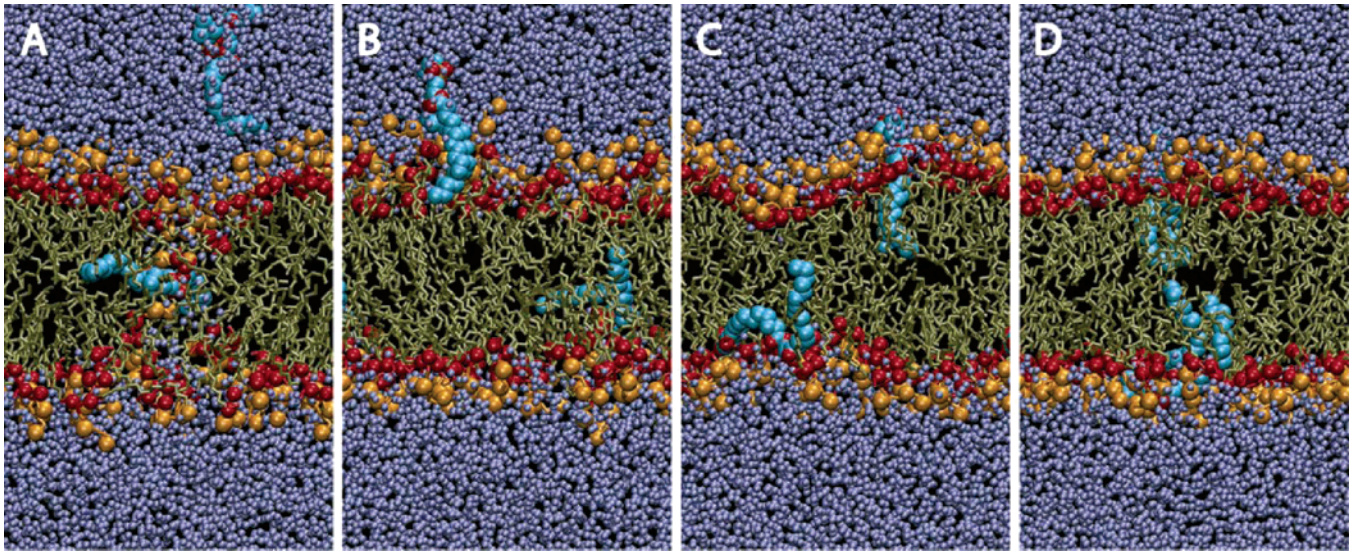

Figure 1. Snapshots of selected simulations: (A) simulation 0, lipid positions 0.0 and −4.0 nm with respect to the center of mass of the bilayer; (B) window 10, lipid positions 0.67 and −3.33 nm; (C) simulation 22, lipid positions 1.47 and −2.53 nm; (D) simulation 29, lipid positions 1.93 and −2.07 nm. Note that the locations of the lipids in simulations 31−60 are symmetric with respect to simulations 0−30. All snapshots are at 50 ns. Graphical representation is denoted by the following: small blue spheres are water oxygen atoms, orange spheres are nitrogen and phosphate, red spheres are oxygens in the lipid glycerol linkage, brown bonds are lipid chains, and the lipids subject to umbrella sampling are in space filling standard colors. Note that the snapshots show all water as well as a small part of the next periodic image in the plane of the membrane to improve the visual representation of the key lipids. Molecular graphics were made with VMD.[52]

of the phosphate group of two lipids independently, one in each leaflet, with a harmonic potential with a force constant of 5000 kJ mol^{-1} nm^{-2}. The two lipids were offset by 4 nm, so that in the first simulation, of the first umbrella window, one lipid was constrained at 0 nm (corresponding to the center of the bilayer) and the second lipid at 4 nm (corresponding to bulk water outside the bilayer). In the remaining 60 simulations both lipids were shifted by 0.067 nm per simulation, corresponding to 61 windows. The 61 starting structures corresponding to the 61 windows were created by pulling the two lipids to their window location using the umbrella potentials with a lower force constant of 500 kJ mol^{-1} nm^{-2} in a 1 ns simulation. Each window was then equilibrated for 10 ns with the full force constant, followed by a 50 ns production simulation. Figure 1 shows a number of snapshots from different umbrella window simulations that illustrate the setup of the system. The system size is ca. $4.7 \times 4.7 \times 9.2$ nm^3. The potential of mean force profile was constructed from the biased distributions of the centers of mass of the lipids using the weighted histogram analysis method[20] with a relative tolerance of 10^{-4}. Thus we have data for two approximately independent lipids (separated by 4 nm, but coupled by the bilayer), which provide a way to estimate errors in the calculations. The force field used is based on OPLS parameters with modifications by Berger et al.[21] Simulations used a 0.9 nm Lennard-Jones and electrostatic cutoff, combined with particle mesh Ewald for long-range electrostatic interactions.[22] A 2 fs time step was used. All bonds in the lipids were constrained using LINCS,[23] all bonds in water using SETTLE.[24] The temperature was controlled using the weak-coupling algorithm, separately to water and lipid with a coupling constant of 0.1 ps and a temperature of 323 K.[25] Pressure was coupled semi-isotropically with a pressure of 1 bar in the *z*-dimension and 1 bar laterally, with a time constant of 2.5 ps.[25]

(18) Berendsen, H. J. C.; Postma, J. P. M.; van Gunsteren, W. F.; Hermans, J. In *Intermolecular Forces*; Pullman, B., Ed.; D. Reidel: Dordrecht, The Netherlands, 1981; pp 331−342.
(19) Torrie, G. M.; Valleau, J. *J. Comp. Phys.* **1977**, *23*, 187−199.
(20) Kumar, S.; Bouzida, D.; Swendsen, R. H.; Kollman, P. A.; Rosenberg, J. M. *J. Comp. Chem.* **1992**, *13*, 1011−1021.
(21) Berger, O.; Edholm, O.; Jahnig, F. *Biophys. J.* **1997**, *72*, 2002−2013.
(22) Essmann, U.; Perera, L.; Berkowitz, M. L.; Darden, T.; Lee, H.; Pedersen, L. G. *J. Chem. Phys.* **1995**, *103*, 8577−8593.
(23) Hess, B.; Bekker, H.; Berendsen, H. J. C.; Fraaije, J. G. E. M. *J. Comp. Chem.* **1997**, *18*, 1463−1472.
(24) Miyamoto, S.; Kollman, P. A. *J. Comput. Chem.* **1992**, *13*, 952−962.
(25) Berendsen, H. J. C.; Postma, J. P. M.; van Gunsteren, W. F.; DiNola, A.; Haak, J. R. *J. Chem. Phys.* **1984**, *81*, 3684−3690.

Results

Figure 1 shows the simulation setup and snapshots from several of the 61 simulation windows. We restrain two lipids that are staggered by 4 nm from the center to the bilayer to bulk water solution at 61 locations and construct the PMF using umbrella sampling. The main result of this study is the lipid PMF, shown in Figure 2A. Figure 2B shows the density distribution of water and lipids, for orientation purposes. The PMF rises steeply for moving lipids deeper into the bilayer and drops smoothly when moving lipids from the bilayer into the water phase. The difference in the PMF near the equilibrium position of the lipid in the bilayer and in the middle of the water phase is ca. 80 kJ/mol. The most important feature of the profile is an abrupt transition to a plateau value at about 3.5−3.9 nm from the center of the bilayer. Because the simulations are symmetric, both sides should give the same result; the difference found is due to sampling errors.

The umbrella simulations allow us to investigate in detail the conformation of lipids at different depths in the membrane. The lipid behavior changes dramatically from the center of the membrane to the water phase. We have chosen to visualize these changes by a simple measure of the compactness of a lipid and by molecular graphics snapshots of lipids at different depths. Figure 3 shows the average distance between the phosphate group center of mass and the center of mass of the last 3 methyl/methylene groups of each tail. Figure 4 shows lipid structures as function of their position in the bilayer in atomistic detail.

The shortest average distance is clearly in the small region of bulk water, where the lipid tails curl up to minimize their water exposure. In the center of the membrane the lipids are also compact, with rapidly changing tail orientations (see Figure 5), with a somewhat larger distance compared to bulk solution. As the lipid is moved from the center of the bilayer to its

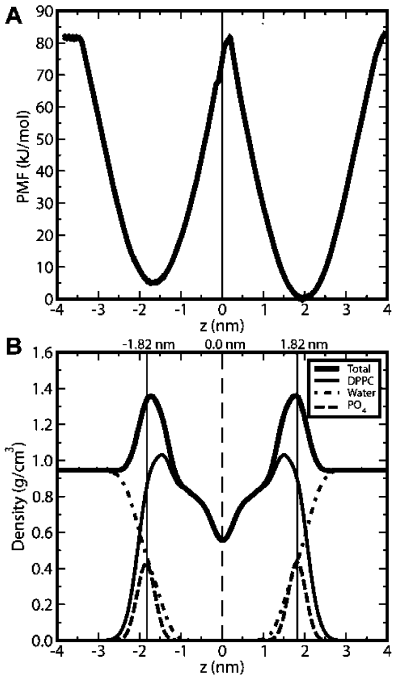

Figure 2. (A) Potential of mean force for a DPPC lipid; (B) density profile for an equilibrium DPPC simulation under the same conditions as the umbrella sampling simulations. The center of the lipid bilayer is at $z = 0$ nm. The thin black lines at -1.82 and $+1.82$ nm indicate the maximum of the equilibrium phosphate group distribution.

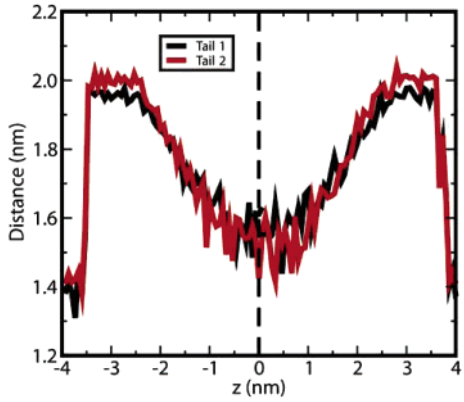

Figure 3. Average distance between the centers of mass of the PO_4 group and the last three carbons of each of the two lipid tails.

equilibrium position (at 1.8−2.0 nm), its tails become increasingly stretched, which continues as the lipid is pulled out of the membrane. The tails are almost completely stretched over a width of ca. 1 nm. A steep drop in lipid length occurs at ca. 4 nm away from the center of the bilayer, and the elongated structure is lost, corresponding to the abrupt change in the potential of mean force as a lipid dissolves in the bulk water.

The lipid head group of DPPC is zwitterionic, with a positive charge on the choline moiety and a negative charge on the phosphate moiety. When this lipid is constrained at the center of the bilayer, a lipid head group with substantial partial charges is embedded in a low-dielectric apolar environment. This results in a major rearrangement of neighboring lipids and water, essentially the formation of a small water pore. Figure 5 shows the molecular details of a few of these pore structures. The constrained head group becomes part of a defect that includes a water file spanning the entire membrane and lipid head groups of adjacent lipids that line this water file.

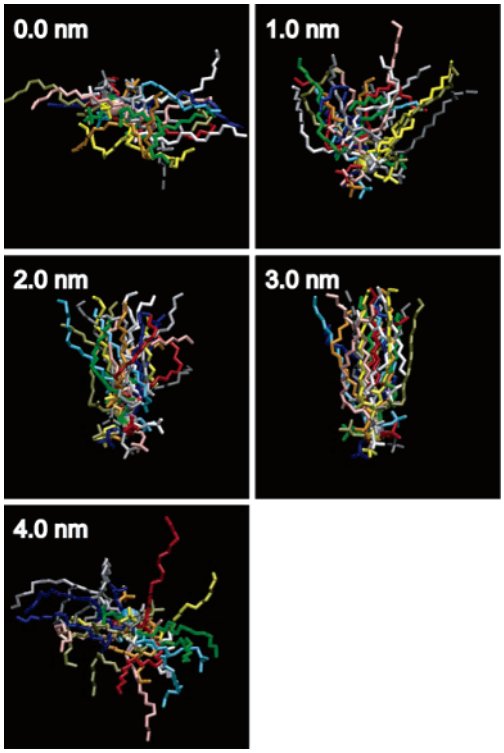

Figure 4. Snapshots of lipids at different locations relative to the center of the membrane: (A) 0.0 nm, (B) 1.0 nm, (C) 2.0 nm, (D) 3.0 nm, (E) 3.6 nm, and (F) 4.0 nm. The center of the membrane is at 0.0 nm, the lipid equilibrium position is at ∼2.0nm, and 4.0 nm is just in bulk water. The simulations extend to 4.0 nm, where the lipid is entirely dissolved in water. Each color indicates a different time, taken from the last 40 ns and separated by 4 ns. Structures are overlaid at the phosphate group by translating them in the plane of the membrane, with no rotations and no translation along the *z*-axis. The yellow solid line indicates the average position of the phosphates of the entire lipid bilayer, the dashed yellow line indicates the center of mass of the entire bilayer.

The lipid tails adopt a broad range of orientations, consistent with the relatively small phosphate-tail distance shown in Figure 3. The snapshots in Figure 5 are chosen to illustrate typical conformations, but when all coordinate sets are examined the water pore is always present, as are neighboring lipid head groups that move deeper into the membrane to line the pore. The pore structure is quite flexible on a nanosecond time scale. For instance, the pore has changed considerably between snapshots C and D, which are separated by only 800 ps.

Discussion

A potential of mean force calculation requires substantial convergence. Although 50 ns for this system is adequate to obtain accurate average structural properties for an entire bilayer, sampling the individual lipids and the response of the bilayer is more difficult. The simulations suffer slightly from incomplete sampling. This is evident from Figures 2 and 4, which have not been symmetrized. If sampling were complete, the free energy difference between the minimum at equilibrium and in solution would be the same for lipids on both sides of the membrane. There actually is a difference of ca. 6 kJ/mol between the two independent lipids, which can be taken as an estimate of the error in the profile. The profile is also not entirely symmetrical around $z = 0.0$ nm. The slowest simulations to equilibrate are the ones with a lipid in the center of the membrane. We checked that the resulting structures are not

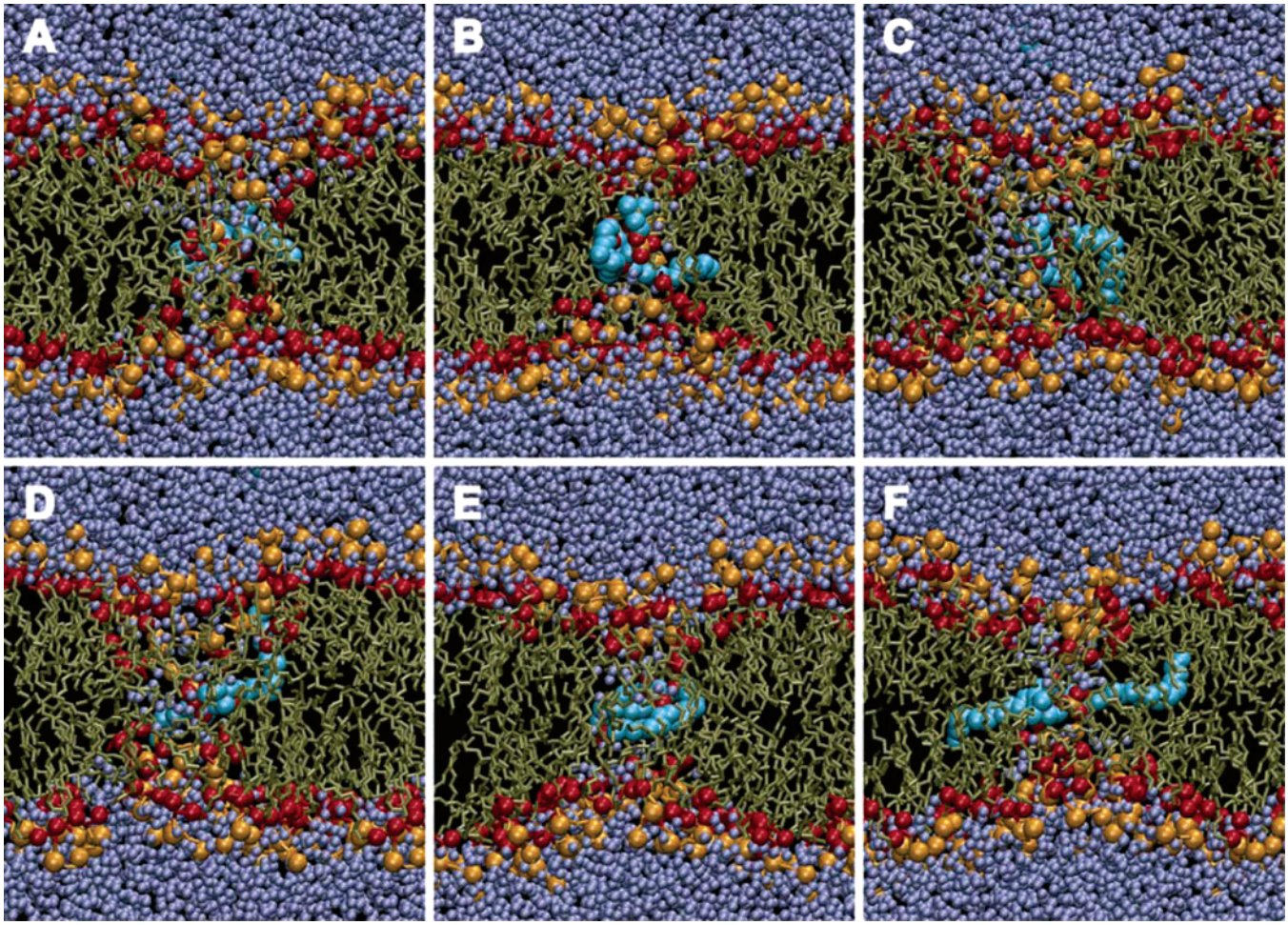

Figure 5. Snapshots of water defects for a lipid constrained in the center of the bilayer. All snapshots are taken from one umbrella window in which one lipid is constrained at the center, the other lipid in bulk water. Panels A−F show snapshots taken at 11.7, 15.7, 31.7, 32.5, 42.4, and 45.1 ns. The rendering is the same as in Figure 1.

artifacts of the starting structures, as simulations starting without this defect equilibrate to the same structure. In one of the two cases with a lipid constrained at the center, initially only half a defect (spanning one membrane leaflet only rather than the entire membrane) forms from one side of the bilayer, but after several ns the defect expands to become similar to those in the snapshots. A second critical part in the profile is the transition between inserted and dissolved acyl chains (Figure 4E). The simulations at this point do sample both extreme orientations. Thus we are confident we have a converged PMF.

The potential of mean force smoothly rises from the equilibrium position of a lipid to bulk water. There is no significant barrier in the profile, but there is an abrupt shift from the steeply rising potential of mean force to a plateau value as the lipid loses contact with the bilayer. In the approach to this point, lipids become increasingly more likely to be fully immersed in water with no contact with the bilayer, even at distances only moderately far away from the bilayer. Forcing lipids deeper into the bilayer than their equilibrium position is very expensive owing to the electrostatic cost of burying the head group charges in a low dielectric environment and is accompanied by the formation of substantial water and lipid defects near the buried lipid. The cost of burying a lipid is comparable to the cost of moving a lipid to bulk solution.

The equilibrium PMF in this paper may be compared with adhesion force energies calculated on essentially the same DPPC system.[26] In nonequilibrium pulling experiments and simulations the energy difference between a lipid in its equilibrium in the membrane and in solution contains a work component.[27] On the basis of the slowest pull rates in ref 26 of 1 nm/ns for the full profile and 0.2 nm/ns for a small part of the profile, we found an initial slow increase in adhesion energy followed by a more rapid rise up to 300 kJ/mol at ca. 3 nm, and a plateau after that. The shape of this profile is similar to the PMF, although the absolute magnitude is 3−4 times too high because of the nonequilibrium contributions to the adhesion energy for a fast pull rate.

The potential of mean force profile cannot be experimentally measured, but we can compare the overall free energy difference between the two extreme states of a lipid in bulk water and a lipid in its equilibrium position in the membrane to the experimentally measured critical micelle concentration (CMC). The CMC of DPPC is 5×10^{-10} M at 298 K.[2] The CMC can be related to an excess chemical potential by

$$\mu - \mu_0 = RT \ln(\mathrm{CMC}) = 323 \times 8.314 \times 10^{-3} \ln(5 \times 10^{-10}/55.5)$$

where the CMC has been converted to mole fraction units. This

(26) Marrink, S. J.; Berger, O.; Tieleman, D. P.; Jahnig, F. *Biophys. J.* **1998**, *74*, 931−943.
(27) Evans, E.; Ritchie, K. *Biophys. J.* **1997**, *72*, 1541−1555.

results in an excess chemical potential of −69 kJ/mol for transfer from solution to the micelle, which we equate with transfer from solution to the bilayer. From the simulations, we obtain a difference between bulk water and the equilibrium position in the membrane of 75−80 kJ/mol at 323 K. The higher temperature in the simulations will affect the CMC but on a free energy scale likely only by a few kJ/mol.[28] This agreement between the simulation and the measured CMC is quite satisfactory given the large energy difference between the two states.

The profile presented here gives the free energy cost of protrusions at different extents. A lipid could be pulled out 0.3 nm for ∼1 kT and 0.4 nm for ∼2 kT, and 1.0 nm requires ∼11 kT. Such protrusions play an important role in several membrane processes. At short distances, local protrusion defects are a significant determinant of the interactions between membranes.[2] Critical material properties such as the high-frequency membrane undulatory and peristaltic bending modes are determined by lipid protrusions.[1] The likelihood of defect formation by single lipids is also an important parameter in models of membrane fusion. In several current models, initial defects form that may consist of individual lipids.[29] The potential of mean force provides an estimate of the likelihood of such defects and for a particular fusion model should provide a reasonably accurate estimate of the probability of a specific degree of exposure of a lipid to the surrounding solvent.

In addition to their role in membrane−membrane interactions, localized lipid defects are likely to play a role in the binding of proteins to membranes, as such interactions depend on the roughness of the interface. This is particularly clear in the action of phospholipase enzymes, some of which only interact with membranes that contain defects.[5] Several other proteins are responsible for carrying lipids between membranes[9] or modifying the lipids enzymatically, which may mean partial removal from the membrane.[5] Although lipids will not dissolve readily by themselves, our results provide estimates of the energetic cost of displacing lipids. This places restrictions on the possible mechanisms of action of proteins that interact with individual lipids. It is feasible to extend the calculations here to include specific types of lipids in a specific background, for example, phosphoinositol lipids that play important roles in signaling.[30]

Our results are for a single lipid in an environment of other lipids, but they are likely to be relevant at least in part for lipids adjusting in the presence of membrane proteins. This is particularly interesting in the context of hydrophobic matching,[31−33] either by lengthening—in effect pulling the lipid phosphate group somewhat out of the membrane—or by shortening the lipid, effectively pushing the lipid deeper into the membrane beyond its equilibrium position in the absence of the perturbing protein. Such defects can be subtle, as in the case of the hydrophobic WALP model peptides,[32] or considerably less subtle, as the defects observed in simulations of charge-containing domains of voltage-gated potassium channels[34] or the action of antimicrobial peptides on the lipid bilayer.[35]

A remarkable result of our simulations is the spontaneous formation of small pores when a lipid is constrained at the center of the bilayer. The structure of these pores is the same as the structure found in other simulations using a variety of methods, including mechanical tension[36,37] and electric fields,[36,38−41] and in spontaneous aggregation of lipids into bilayers and vesicles.[13,42] We are now able to calculate the free energy of the formation of such small pores in a detailed atomistic model, which has been done previously by other methods for pores in highly simplified membrane models.[43,44] Recently, Wohlert et al. calculated the free energy of pore formation in a DPPC bilayer using a parameter related to pore radius as reaction coordinate, finding values in the range of 75−100 kJ for small pores,[45] which is of similar magnitude to the value of 80 kJ/mol we obtain.

On the basis of this result, we can estimate the average number of pores per surface area of membrane and, with some additional assumptions and results from other simulations, the rates of formation and dissipation of the pores as well as the permeation rate of lipids and other molecules through a membrane by passive diffusion through pores.

First, we calculate the equilibrium number of pores per area. The pore density ρ is given by $\rho = \exp(-\Delta G_{pore}/kT)/A_{lip} = 18$ pores per cm^2, or ca. 5 10^{-8} pores for a spherical liposome with a diameter of 1 micrometer, using $\Delta G_{pore} = 80$ kJ/mol. With $\Delta G_{pore} = 75$ kJ/mol, the pore density becomes 120 pores per cm^2. The equilibrium pore density, in the absence of an external electric field, also occurs in models of electroporation.[46,47] These models use a broad range of equilibrium pore densities, with a lower bound of ca. 50 pores per cm^2.[47] Thus our equilibrium pore density appears quite reasonable, as pure DPPC may be particularly stable against water defect formation compared to biological cell membranes.

Next, we calculate the pore formation time. The rate constants k_f for pore formation and k_d for pore dissipation are related by the free energy cost of pore formation:

$$\frac{k_f}{k_d} = \exp(-\Delta G_{pore}/kT)$$

The constant k_d can be estimated from simulations in which pores were created and their time evolution followed. Previous simulations found pore life times of 10−100 ns.[13,42] With $\Delta G_{pore} = 80$ kJ/mol and $k_d = 10^7-10^8$ s^{-1}, we find $k_f = 10^{-6}-10^{-7}$

(28) Majhi, P. R.; Blume, A. *Langmuir* **2001**, *17*, 3844−3851.
(29) Chernomordik, L. V.; Kozlov, M. M. *Annu. Rev. Biochem.* **2003**, *72*, 175−207.
(30) McLaughlin, S.; Wang, J. Y.; Gambhir, A.; Murray, D. *Annu. Rev. Biophys. Biomol. Struct.* **2002**, *31*, 151−175.
(31) Mouritsen, O. G.; Bloom, M. *Biophys. J.* **1984**, *46*, 141−53.
(32) de Planque, M. R.; Killian, J. A. *Mol. Membr. Biol.* **2003**, *20*, 271−284.
(33) Killian, J. A.; von Heijne, G. *Trends Biochem. Sci.* **2000**, *25*, 429−434.
(34) Freites, J. A.; Tobias, D. J.; von Heijne, G.; White, S. H. *Proc. Natl. Acad. Sci. U.S.A.* **2005**, *102*, 15059−15064.
(35) Epand, R. M.; Vogel, H. J. *Biochim. Biophys. Acta* **1999**, *1462*, 11−28.
(36) Tieleman, D. P.; Leontiadou, H.; Mark, A. E.; Marrink, S. J. *J. Am. Chem. Soc.* **2003**, *125*, 6382−6383.
(37) Leontiadou, H.; Mark, A. E.; Marrink, S. J. *Biophys. J.* **2004**, *86*, 2156−2164.
(38) Tarek, M. *Biophys. J.* **2005**, *88*, 4045−4053.
(39) Tieleman, D. P. *BMC Biochem.* **2004**, *5*, 10.
(40) Gurtovenko, A. A.; Vattulainen, I. *J. Am. Chem. Soc.* **2005**, *127*, 17570−17571.
(41) Vernier, P. T.; Ziegler, M. J.; Sun, Y.; Chang, W. V.; Gundersen, M. A.; Tieleman, D. P. *J. Am. Chem. Soc.* **2006**, *128*, 6288−6289.
(42) Marrink, S. J.; Lindahl, E.; Edholm, O.; Mark, A. E. *J. Am. Chem. Soc.* **2001**, *123*, 8638−8639.
(43) Tolpekina, T. V.; den Otter, W. K.; Briels, W. J. *J. Chem. Phys.* **2004**, *121*, 12060−12066.
(44) Wang, Z. J.; Frenkel, D. *J. Chem. Phys.* **2005**, 123, 154701.
(45) Wohlert, J.; den Otter, W. K.; Edholm, O.; Briels, W. J. *J. Chem. Phys.* **2006**, 124, 154905.
(46) Smith, K. C.; Neu, J. C.; Krassowska, W. *Biophys. J.* **2004**, *86*, 2813−2826.
(47) Gowrishankar, T. R.; Esser, A. T.; Vasilkoski, Z.; Smith, K. C.; Weaver, J. C. *Biochem. Biophys. Res. Commun.* **2006**, *341*, 1266−1276.

s^{-1}. This is the rate of pore formation per lipid. We can calculate the rate of pore formation per unit area in cm^2, assuming an area per lipid of 0.64 nm^2, $k_f = 10^{-6}-10^{-7}/(0.64 \times 10^{-14}\ cm^2\ s)$. For the liposome above, we find that an average of 0.5−5 pores form spontaneously per second, with a pore life time of 10−100 ns.

On the basis of the pore density ρ, we can calculate the flux of lipids and other molecules through the pore defects. The total flux of particle i through the membrane, using pores, is

$$J_i = j_i \rho$$

with J_i the total flux (particles per second per cm^2), j_i the flux through the pore (particles per second), and ρ the pore density (pores per cm^2). We will use 10^2 pores per cm^2, realizing this value is sensitive to uncertainties in the free energy barrier for defect formation. We can estimate j_i for a number of types of i from other simulations.

Water. Leontiadou et al. found that for small pores at low membrane tension, the water flux is 6 water molecules per nanosecond.[37] Thus $j_{water} \approx 10^{10}\ s^{-1}$, which gives $J_{water} \approx 10^{12}$ particles $cm^{-2}\ s^{-1}$, or of the order of 10^4 water molecules per second for the liposome.

Lipids. In simulations of the spontaneous formation of a vesicle, lipid flip-flop is observed across the edge of pore defects on a 5−10 ns time scale.[13] Using 10 ns, this corresponds to $j_{lipid} \approx 10^8\ s^{-1}$, which gives $J_{lipid} \approx 10^{10}$ particles $cm^{-2}\ s^{-1}$, or ca. 10^2 lipid molecules per second for the liposome. Per lipid area of $0.64\ 10^{-14}\ cm^2$, this corresponds to 10^{-5} flips per second, or an average life time in the same leaflet of 10^5 s or ca. 30 h.

Sodium. Leontiadou et al. found that for small pores at low membrane tension, the sodium flux is ca. 4 sodium ions per 100 ns.[48] Thus $j_{Na^+} \approx 10^7\ s^{-1}$, which gives $J_{Na^+} \approx 10^9$ particles $cm^{-2}\ s^{-1}$, or ca. 10 sodium ions per second for the liposome.

From the flux data we can obtain permeability coefficients P, with

$$P_i = \frac{J_i}{\Delta C}$$

with P in cm/s and ΔC the driving concentration difference. In the symmetric case, there is no concentration difference and we consider the unidirectional flux only. We find for water, with $\Delta C = 55$ M, P $\approx 10^{-11}$ cm/s; for lipids, with $\Delta C = 1/(0.5\ dA_{lip})$ (corresponding to 1 lipid per $V_{lip} = 1.2\ nm^3$) P $\approx 10^{-11}$ cm/s; and for sodium, with $\Delta C = 0.2$ M (the concentration used in[47]) P $\approx 10^{-13}$ cm/s.

These numbers show that water permeation through a pore makes a negligible contribution to water permeation through membranes. The experimental value for water permeation is of the order of $P = 10^{-4}$ cm/s, 7 orders of magnitude faster than what we find for permeation through pores only. Indeed, calculated water permeation rates based on free energy calculations of a water molecule at different locations in the membrane predict exactly that water permeation occurs without major defects.[49] Lipids have a surprisingly high permeation rate, comparable to that of ions. We predict flip-flop of lipids to occur on a time scale of 10^5 seconds (ca. 30 h), in good agreement with experimental measurements that span a range from 1 to 90 h depending on specific experimental conditions, in particular the type of vesicles used.[12,50,51] This time scale depends strongly on the free energy barrier for defect formation. Using our lower value of 75 kJ/mol (ca. 2 kT lower), the flip-flop time becomes 4 h. Finally, sodium ions have a permeation rate through pores that is comparable to the experimentally measured permeation rate of sodium through pure lipid bilayers of $P = 10^{-12}-10^{-14}$ cm/s.[14] Therefore, our results strongly suggest that sodium permeation—and likely permeation of other ions—occurs through water pore defects. Toyoshima and Thompson measured the thermodynamics of radioactive chloride flux,[15] showing that the process had the same activation barrier as lipid flip-flop.[12] They concluded that transport of chloride ions probably occurred through the same defects as lipid flip-flop. Our simulations provide a detailed structural conformation of this idea. In previous simulations of the potential of mean force for unassisted sodium and chloride transport across glycerol 1-monooleate, Wilson and Pohorille found substantial defects similar to the ones observed here, although these defects did not span the full bilayer.[52,53] This suggests that the exact nature of the defects may depend on the lipid chain length[54] and the nature of the head groups. 1-Monooleate has a substantially less polar headgroup compared to DPPC. It will also be interesting to extend this work to include bilayer modifiers such as cholesterol, small molecules, external electric fields, and membrane proteins. The latter may be of particular biological importance. Recent experiments have shown that lipid flip-flop is greatly accelerated by the presence of some alpha-helical membrane proteins that do not have specific transport capabilities, including synthetic peptides.[55] On the basis of our simulations we speculate that this is due a much lower barrier for defect formation, including water penetration, while similar features as observed in Figure 5 are maintained. This could be tested by further simulations.

Acknowledgment. This work was supported by the Natural Science and Engineering Research Council. DPT is an Alberta Heritage Foundation for Medical Research Senior Scholar, CIHR New Investigator, and Sloan Foundation Fellow. Calculations were done on WestGrid computers. We thank Tom Vernier for his comments.

JA0624321

(48) Leontiadou, H. *Modeling Membranes under Stress*; University of Groningen: Groningen, The Netherlands, 2005.

(49) Marrink, S. J.; Berendsen, H. J. C. *J. Phys. Chem.* **1994**, *98*, 4155−4168.
(50) Wimley, W. C.; Thompson, T. E. *Biochem.* **1990**, *29*, 1296−1303.
(51) De Kruijff, B.; Van Zoelen, E. J. *Biochim. Biophys. Acta* **1978**, *511*, 105−115.
(52) Wilson, M. A.; Pohorille, A. *J. Am. Chem. Soc.* **1996**, *118*, 6580−6587.
(53) Pohorille, A.; Wilson, M. A. *Cell. Mol. Biol. Lett.* **2001**, *6*, 369−374.
(54) Deamer, D. W.; Volkov, A. G. *Bioelectrochem. Bioenerg.* **1997**, *42*, 153−160.
(55) Kol, M. A.; van Dalen, A.; de Kroon, A.; de Kruijff, B. *J. Biol. Chem.* **2003**, *278*, 24586−24593.